



# Learning from nature: constructing high performance graphene-based nanocomposites

**Shanshan Gong<sup>1</sup>, Hong Ni<sup>1</sup>, Lei Jiang and Qunfeng Cheng\***

Key Laboratory of Bio-inspired Smart Interfacial Science and Technology of Ministry of Education, School of Chemistry and Environment, Beihang University, Beijing 100191, PR China

After billions of years of evolution, natural materials, such as bamboo, bone, and nacre, show unique mechanical properties, due to their intrinsic hierarchical micro/nanoscale architecture and abundant interfacial interactions. This relationship between architecture, interfacial interactions, and mechanical properties of natural materials, supplies the inspiration for constructing high performance lightweight nanocomposites. Graphene's high tensile strength, Young's modulus, and electrical conductivity when compared with other nanomaterials make it an ideal building block for constructing high performance bioinspired nanocomposites. Such nanocomposites demonstrate promise for applications in many fields, including aerospace, aeronautics, submarine devices, car, and flexible electronic devices. In this review, we focus on the bioinspired strategy for preparing graphene-based nanocomposites (GBNs), and discuss the various interfacial interactions. Then the synergistic effects from building blocks and interfacial interactions are discussed in detail, along with the resultant GBNs used in the applications of sensors, actuators, supercapacitors, and nanogenerators, are also illustrated. These GBNs include, for example, one-dimensional (1D) fiber, two-dimensional (2D) film, and three-dimensional (3D) bulk nanocomposites. Finally, we provide our perspective on GBNs, and discuss how to efficiently mimic natural materials for creating new multifunctional bioinspired nanocomposites for practical applications in the near future.

## Introduction

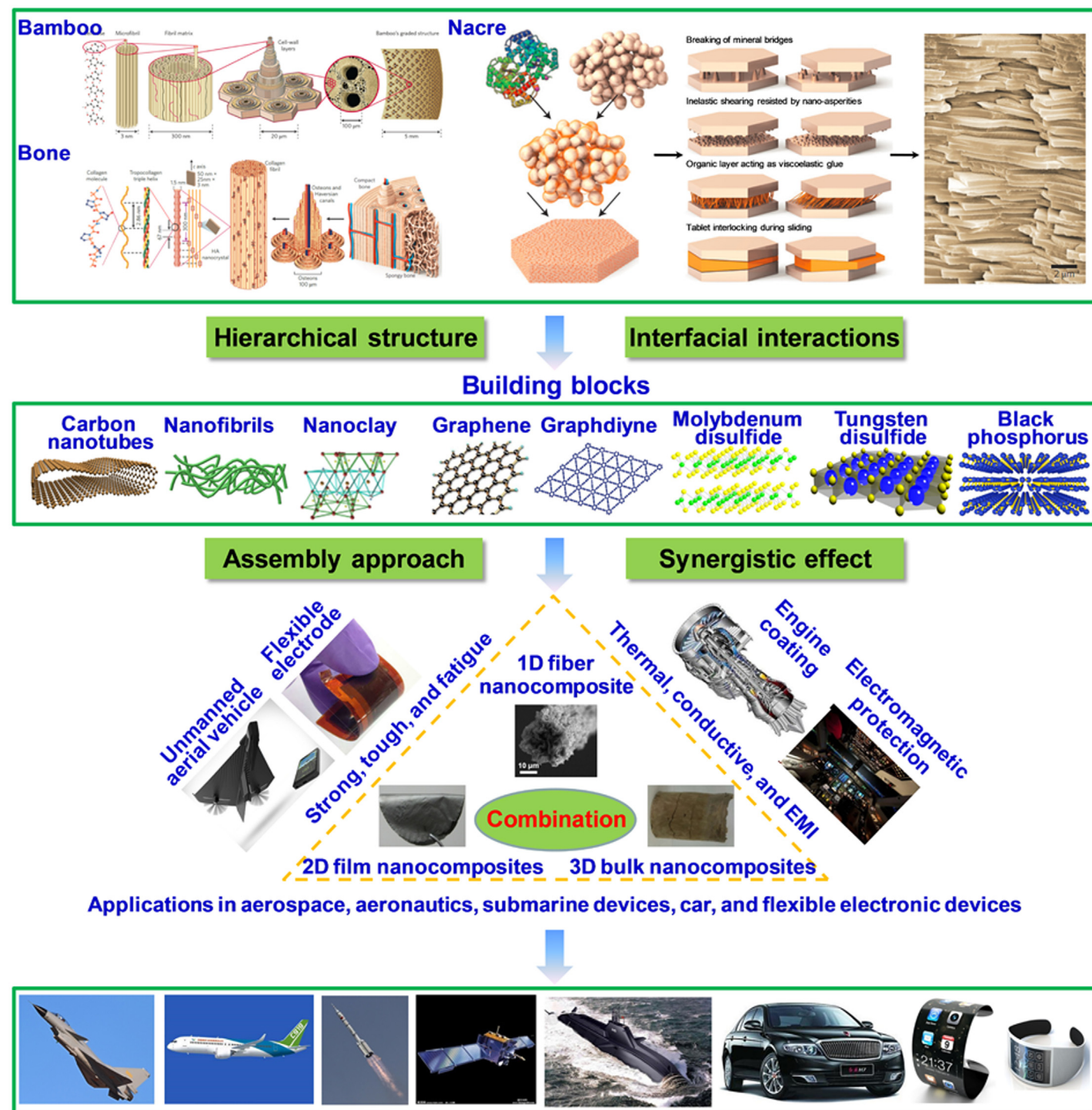
There are many reviews on bioinspired materials, including surface [1], interface [2], intelligent, and bulk materials [3]. However, few reviews discuss the process of creating bioinspired nanocomposites, including achieving inspiration from nature, selecting building blocks, assembling nanocomposites, and demonstrating these nanocomposites' applications. In this review, we propose a research roadmap on how to learn from nature and fabricate graphene-based nanocomposites (GBNs) based on our and other groups' work, as shown in Fig. 1. Natural materials [4], such as bamboo, bone, and nacre, show unique mechanical properties, including high strength, toughness, and fatigue properties.

Research has discovered that there are typical hierarchical micro/nanoscale architecture and abundant interfacial interactions in natural materials, which provide promising inspiration for constructing high performance nanocomposites.

Recent research on nanomaterials makes use of many building blocks for preparing nanocomposites with extraordinary mechanical properties, including 1D carbon nanotubes, nanofibrils, and 2D nanoclay, graphene, graphdiyne, molybdenum disulfide, tungsten disulfide, and black phosphorus. These nanomaterials are ideal candidates for preparing bioinspired nanocomposites through different assembly approaches, such as 1D fiber nanocomposites [5–8], 2D film nanocomposites [2,9–12], and 3D bulk nanocomposites [13,14]. Integrated excellent mechanical properties can be achieved via synergistic toughening. For example, Zhang et al. [15] created ultrastrong graphene fiber nanocomposites with tensile strength of

\*Corresponding author: Cheng, Q. (cheng@buaa.edu.cn)

<sup>1</sup>These authors contributed equally to this work.

**FIGURE 1**

A schematic illustration of GBNs from fabrication to potential applications. First, the inspirations, extracted from natural materials, such as bamboo, bone, and nacre, are a hierarchical micro/nanoscale architecture and abundant interfacial interactions, which work as the principles for enhancing the mechanical properties of resultant GBNs. Reproduced from Ref. [4] with permission from Copyright © 2015 Nature Publishing Group. Second, the different nanomaterials, including 1D carbon nanotubes, nanofibrils, 2D nanoclay, graphene, graphdiyne, molybdenum disulfide, tungsten disulfide, and black phosphorus, are typically chosen as building blocks to be assembled into new high performance GBNs via different approaches and synergistic effects. Third, the physical performance of GBNs, including 1D fiber, 2D film, and 3D bulk nanocomposites, are tuned through different assembly approaches and synergistic effects to obtain high mechanical, electrical, thermal, conductive, and EMI properties. Finally, these high performance GBNs could be utilized in aerospace, aeronautics, submarine devices, car, and flexible electronic devices in the near future.

842.6 MPa via synergistic interfacial interactions of ionic and covalent bonding. Xiong et al. [16] fabricated ultrastiff graphene film nanocomposites with Young's modulus of 169 GPa by introducing cellulose nanocrystals to form a synergistic effect from different building blocks, and Shin et al. [17] prepared super tough graphene-based fiber nanocomposites with toughness of 1380 MJ/m<sup>3</sup> via synergistic toughening of single-walled carbon nanotubes. In addition, carbon fiber and carbon nanotubes were assembled into hybrid nanocomposites with integrated high mechanical and electrical properties, which have been used for constructing a commercial unmanned aerial vehicle [18]. GBNs have been also applied as electrodes in flexible electronic devices [19]. 3D printed reduced graphene oxide (rGO)-based heaters with different shapes can be directly printed onto different substrates to enable heating anywhere, due to their high performance thermal supply with a high temperature and ultrafast heating rate of ~20,000 K/s [20]. Highly thermal and electrical conductive rGO fibers with 1290 W/(m K) and  $2.21 \times 10^3$  S/cm have been fabricated through thermal annealing at 2850°C [21], which can be used as electromagnetic interference (EMI) shielding on the electronic instrument for electromagnetic protection. Furthermore, these GBNs show promise for applications in the fields of aerospace, aeronautics, submarine devices, car, and flexible electronic devices.

### Inspiration from nature

Nacre demonstrates the unique relationship between mechanical properties and brick-and-mortar architecture [4]. Nacre (abalone shell, Fig. 2a) is made of at least 95 vol% inorganic aragonite and at most 5 vol% organic matrix. The 'bricks' of mineral polygonal tablets, with a thickness of 200–500 nm and diameter of 5–10 μm are mesocrystals assembled from nanograins with organic materials (Fig. 2b) [22]. The 'mortar' refers to the protein matrix (Fig. 2c) [22], including different organic components [23], such as chitin, lustrin A, and Pif97. This unique hierarchical micro/nano-scale architecture and these abundant interfacial interactions play key roles in mechanical properties of nacre. The fracture toughness of nacre is 3000 times higher (in energy terms) than that of aragonite (Fig. 2d) [24], indicating an 'amplification effect' in mechanical properties beyond the rule of mixtures in traditional composites (Fig. 2e) [4]. The amplification effect in nacre has been subject of many studies and is attributed to the fine nacre architecture and optimized hard/soft interfaces. But little progress has been made in addressing the challenges in developing theoretical models to explain the amplification effect beyond the rule of mixtures.

Although the interfaces occupy a small volume fraction in nacre, the deformation and fracture of nacre are largely governed by interfaces. The organic interface in nacre is shown in Fig. 2f [23], consisting of a layer of chitin fibrils and many kinds of proteins. In addition, there are many different interactions, such as hydrogen, covalent, and ionic bonds between proteinaceous layers and aragonite [23]. This kind of interface usually works in synergy with the sophisticated architecture of nacre via inelastically deforming, redistributing stresses around defects, and deflecting crack propagations [23].

Since the discovery of the unique properties of nacre in 1988 [25], almost 30 years of investigation have provided two materials design principles: (i) assemble an orderly hierarchical micro/nanoscale inorganic–organic architecture with a high

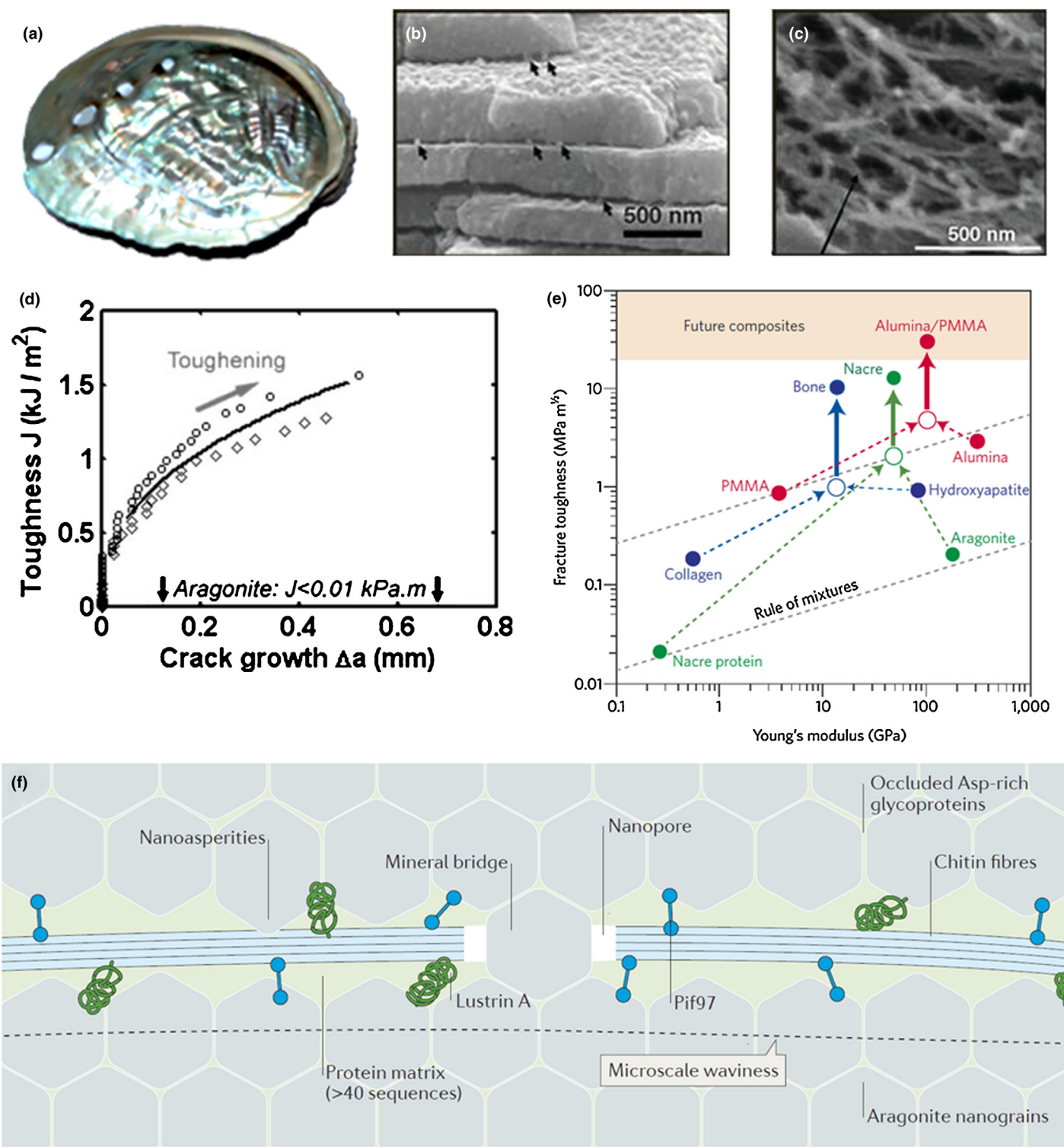
volume fracture of inorganic components; (ii) design abundant interfacial interactions of non-covalent and covalent bonding. The unique architecture and interfacial interactions of nacre result in a mechanical amplification effect, which is larger than that of the rule of mixtures [4]. Thus, these principles, which are discussed in detail in the following two sections, are crucial in designing nacre-like nanocomposites.

### Mechanical properties of building blocks

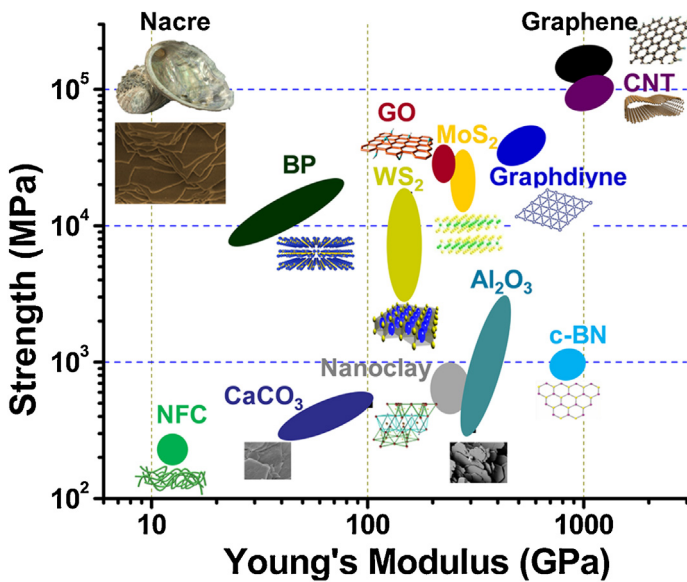
The aim of discovering the unique properties of natural nacre is to obtain the inspiration for constructing novel high performance nanocomposites. Thus, the performance of the building blocks is essential for enhancing the assembled bioinspired nanocomposites. Figure 3 compares the mechanical properties, including strength and Young's modulus, of a series of building blocks used for mimicking nacre in nanocomposite design. These building blocks include nanofibrillar cellulose (NFC) [26,27], man-made calcium carbonate (CaCO<sub>3</sub>) [28], nanoclay [29], aluminum oxide (Al<sub>2</sub>O<sub>3</sub>) [30], layered double hydroxides (LDH) [31], tungsten disulfide (WS<sub>2</sub>) [32], molybdenum disulfide (MoS<sub>2</sub>) [33], flattened double-walled carbon nanotubes [34], cubic boron nitride (c-BN) [35], graphene oxide (GO) [36], graphene [37], graphdiyne [38], and black phosphorus (BP) [39]. Man-made CaCO<sub>3</sub> platelets, genuine chemical components similar to natural nacre, showed a tensile strength of 334–505 MPa [30] and Young's modulus of 50–100 GPa [40]. Bioinspired nanocomposites based on CaCO<sub>3</sub> were demonstrated by Li et al. [28]. However, the maximum ultimate strength was only 97 MPa, lower than that of natural nacre [25]. This is because of weak interfacial interactions between CaCO<sub>3</sub> platelets and gelatine.

Compared with CaCO<sub>3</sub> platelets, nanoclay shows much higher mechanical properties with a tensile strength of 500–700 MPa [41], and Young's modulus of 400 GPa [42]. In addition, nanoclay with functional groups on its surface can be also covalently cross-linked with a polymer matrix, resulting in a strong interface. For example, Podsiadlo et al. [29] demonstrated ultrastiff bioinspired nanocomposites based on nanoclay and poly vinyl alcohol (PVA) via covalent cross-linking, demonstrating Young's modulus up to 107 GPa. Studart et al. [30] fabricated super tough bioinspired nanoclay/chitosan nanocomposites with a toughness of 75 MJ/m<sup>3</sup> via constructing hydrogen bonding networks between adjacent nanoclay platelets. Al<sub>2</sub>O<sub>3</sub> platelets with a tensile strength of 330–2000 MPa and Young's modulus of 300–400 GPa were assembled into bioinspired nanocomposites with polymethyl methacrylate (PMMA) by Munch et al. [43]. Bioinspired Al<sub>2</sub>O<sub>3</sub>/PMMA nanocomposites had an exceptional fracture toughness of 30 MPa m<sup>1/2</sup>, which is more than 300 times that of their constituents.

Recently, transition metal sulphides such as WS<sub>2</sub> and MoS<sub>2</sub> platelets were successfully fabricated by liquid exfoliation [32]. The mechanical properties of individual WS<sub>2</sub> nanotubes were tested in a high-resolution scanning electron microscope [44]. The tensile strength and Young's modulus reached up to 3.7–16.3 GPa and 152 GPa, respectively. The other typical transition metal sulphide of MoS<sub>2</sub> also showed high mechanical properties with a tensile strength of 16–30 GPa and Young's modulus of 270 GPa [45]. Recently, MoS<sub>2</sub> nanosheets were assembled with GO into ternary artificial nacre nanocomposites by Wan et al. [33], showing integration of high strength and toughness. Chan et al. [46] investigated

**FIGURE 2**

Natural nacre, with its extraordinary properties, supplies a unique inspiration for constructing GBNs. (a) Digital image of abalone nacre. (b) 95 vol% CaCO<sub>3</sub> platelets are assembled into layered structure. (c) Only 5 vol% protein and chitin are utilized for bonding the CaCO<sub>3</sub> platelets. Reproduced from Ref. [22] with permission from Copyright © 2013 The American Association for the Advancement of Science. (d) The fracture toughness of nacre is 3000 times higher than that of single CaCO<sub>3</sub> platelet. Reproduced from Ref. [24] with permission from Copyright © 2009 Elsevier. (e) The hierarchical micro/nanoscale architecture and abundant interfacial interactions of bone and nacre amplify the toughening effect more highly than the rule of mixtures, which is demonstrated in the bioinspired Al<sub>2</sub>O<sub>3</sub>/PMMA nanocomposites. Reproduced from Ref. [4] with permission from Copyright © 2015 Nature Publishing Group. (f) The interfacial interactions of nacre can be schematically illustrated as follows: protein matrix, mineral bridge, nanopore, pif97, lustrin A, and chitin fibers. Reproduced from Ref. [23] with permission from Copyright © 2016 Nature Publishing Group.

**FIGURE 3**

Mechanical properties comparison of different nanomaterials in tensile strength and Young's modulus. These nanomaterials are usually chosen as building blocks for constructing bioinspired nanocomposites. Obviously, graphene and its derivative, water-soluble GO, demonstrate an integrated strength and Young's modulus superior to other nanomaterials, including NFC, CaCO<sub>3</sub>, nanoclay, Al<sub>2</sub>O<sub>3</sub>, BP, MoS<sub>2</sub>, WS<sub>2</sub>, c-BN, carbon nanotubes, and graphdiyne nanoplatelets. Thus, graphene and GO are ideal candidates for preparing GBNs.

the mechanical properties of c-BN film via nanoindentation, and the Young's modulus reached up to 800 GPa. A new two-dimensional nanomaterial of black phosphorus (BP) was also investigated through adopting classical molecular dynamics simulations [47], and the theoretically calculated tensile strength and Young's modulus were 334–505 MPa and 50–100 GPa, respectively. Recent investigations reveal that carbon nanomaterials, such as carbon nanotubes, GO, graphene, and graphdiyne, are attractive building blocks for constructing bioinspired nanocomposites. Carbon nanotubes exhibit a tensile strength of about 100 GPa and a Young's modulus of about 1000 GPa [48]. Graphene nanosheets show a much higher tensile strength of about 130 GPa, and a Young's modulus of about 1000 GPa [49], which is superior to the water-soluble derived GO nanosheets with a tensile strength of 20–30 GPa and a Young's modulus of 240 GPa [50–55], due to oxygen-contained functional groups on their surface. Graphdiyne, a new graphene derivative material, also shows an ultimate tensile strength of 36–46 GPa and Young's modulus of 470–580 GPa calculated by a theoretical model [56].

Based on the intrinsic mechanical properties of nanomaterials listed in Fig. 3, carbon-based nanomaterials are ideal candidates for preparing GBNs, especially for the graphene derivative GO. This is because of a large amount of functional groups on the surface of GO, including hydroxyl, carboxylic, and epoxide groups [57], which make it easy to design different interfacial interactions with all kinds of organic matrix. In the following section, the interface design in GBNs is discussed in detail. It should be noted that the geometry of building blocks also shows great effect on the mechanical properties of bioinspired nanocomposites [58–60]. However, the size of GO nanosheets is very difficult to control in the

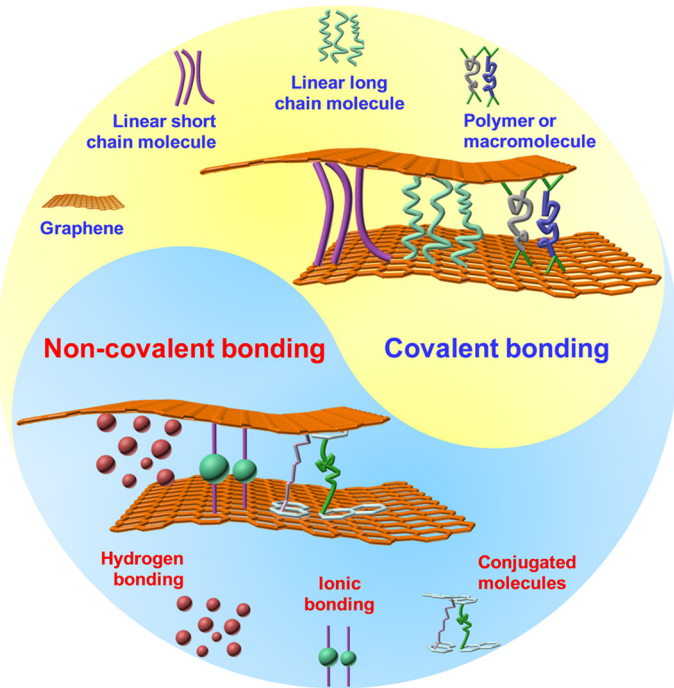
synthesis process using Hummers method. Thus, this review focuses on interfaces of graphene-based nanocomposites.

### Interfacial interactions

Interfacial interactions in natural materials play a large role in determining resultant mechanical properties. Inspired by these interfacial interactions, many different kinds of interfacial interactions have been constructed to improve the mechanical properties of GBNs. These interactions can be divided into two categories: (i) non-covalent bonding and (ii) covalent bonding, as shown in Fig. 4. Non-covalent bonding and covalent bonding usually synergistically work together in enhancing mechanical properties, resulting in an amplification effect. The essence of synergistic toughening effect is to simultaneously maximize the enhancement of the weak non-covalent and strong covalent bonding thus improving the mechanical properties of GBNs.

#### Non-covalent bonding

Non-covalent bonding, including hydrogen bonding, ionic bonding, and  $\pi-\pi$  interactions, usually shows relatively weak strength compared with covalent bonding. However, the mechanical properties of GBNs have been enhanced via non-covalent bonding due to their easy construction with graphene nanosheets. For example, Dikin et al. [36] fabricated GO paper with a tensile strength of 133 MPa and Young's modulus of 32 GPa. The high mechanical

**FIGURE 4**

Two kinds of interfacial categories in GBNs: non-covalent bonding and covalent bonding. Non-covalent bonding, which is relatively weaker than covalent bonding contains the hydrogen bonding, ionic bonding, and  $\pi-\pi$  interactions. The strength of resultant GBNs can be not only dramatically enhanced by covalent bonding, but also the toughness could be tuned by controlling the molecule chain of covalent cross-linking. In fact, non-covalent and covalent bondings work together in GBNs, resulting in a synergistic effect. The enhancement of mechanical properties is further amplified, higher than sum of independent non-covalent and covalent bonding.

properties are attributed to hydrogen bonding between adjacent GO nanosheets and water molecules. Molecular dynamic simulations revealed that hydrogen bonding was formed not only between functional groups on adjacent GO nanosheets, but also between GO nanosheets and water molecules [61]. Thus, the mechanical properties of GBNs can be improved via increasing the number of hydrogen bonding networks. Putz et al. [62] demonstrated high density of hydrogen bonding networks by introducing the organic polymer, poly(vinyl alcohol) (PVA), with hydroxyl groups or oxygen groups. The results show that the Young's modulus of bioinspired GO-PVA nanocomposites with GO content of 77.4 wt% reaches up to 36.3 GPa. The tensile strength of bioinspired GO-PVA nanocomposites with GO content of 80 wt% is as high as 188.9 MPa [63]. The results of joint experimental, theoretical, and computational simulation revealed that this further enhancement can be attributed to cooperative interactions of hydrogen bonding networks between PVA and GO nanosheets, and between water molecules and GO nanosheets [64].

On the other hand, metal ionic bonding also results in outstanding mechanical properties in natural materials [2], such as zinc, copper, manganese, calcium, titanium, aluminum, and iron. Park et al. [65] incorporated calcium and magnesium into GO paper to construct ionic bonding between adjacent GO nanosheets via two modes of interactions: (i) bridging the edges of GO nanosheets and (ii) intercalating between the basal planes. The experimental results revealed that the bridging mode is stronger than the intercalating mode. The  $\pi-\pi$  interactions between graphene nanosheets are usually formed via conjugated molecules with pyrene derivatives. For example, Xu et al. [66] demonstrated the effect of  $\pi-\pi$  interaction on improving the mechanical properties of GBNs via 1-pyrenebutyrate. Compared with hydrogen and ionic bonding, the  $\pi-\pi$  interactions show a great advantage of simultaneously enhancing interfacial strength and the electrical conductivity of resultant GBNs.

Recently, a series of pyrene derivatives were demonstrated to enhance the plane-to-plane tunneling conductivity of GBNs [67]. Furthermore, pyrene molecules grafted with a linear long chain polymer were also developed for tuning the mechanical properties of resultant GBNs, such as pyrene molecules with a functional segmented poly(glycidyl methacrylate) [68], and functionalized polyethylene glycol with pyrene groups [69]. The experimental results reveal that pyrene grafted with linear chain molecules is better for enhancing mechanical properties via  $\pi-\pi$  interactions.

### Covalent bonding

While covalent bonding shows strong interfacial strength, it can also be tuned by adjusting the length of the molecule chain and density of cross-linking. Using the small molecules as cross-linkers usually enhances strength and stiffness but results in relatively low toughness, due to the restriction of sliding between adjacent graphene nanosheets. For example, glutaraldehyde was utilized to cross-link GO nanosheets via reacting with hydroxyl groups on the surface of GO nanosheets through intermolecular acetalization [70], resulting in improvements of 59% and 190% in tensile strength and Young's modulus, respectively, of resultant GBNs. Another example is borate cross-linked GO nanocomposites via borate oligo-orthoesters between adjacent GO nanosheets [71].

The modulus of borate-GO nanocomposites was improved from 30 GPa to 127 GPa. Although the Young's modulus was greatly enhanced, the toughness was not simultaneously improved.

Recent investigations reveal that long chain linear molecules are better for enhancing tensile strength and toughness. For instance, Cheng et al. [10] utilized a long chain linear molecule of 10,12-pentacosadiyn-1-ol (PCDO) to cross-link the adjacent GO nanosheets via esterification reaction between the alcohol groups at one end of the PCDO and the carboxylic acids on the surface of the GO nanosheets. The toughness of rGO-PCDO nanocomposites was improved to 3.9 MJ/m<sup>3</sup>, about two times higher than that of natural nacre [25]. Compared with long chain linear molecules, a polymer or macromolecules with active functional groups can achieve integrated strength, stiffness, and toughness, due to their high density of covalent cross-linking. For example, Cui et al. [72] demonstrated poly(dopamine) (PDA) cross-linking GO nanosheets with a high density of covalent bonding, resulting in both improvement in tensile strength and toughness of rGO-PDA nanocomposites. In nacre, there are complicated interfacial interactions, including non-covalent and covalent bonding together [23]. These different kinds of interactions usually work synergistically together, resulting in excellent integrated mechanical properties.

### Synergistic effect

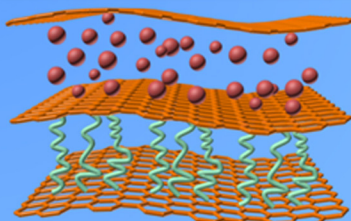
Natural materials, such as bamboo, wood, and bone, reveal that unique mechanical properties usually depend on synergistic effects from interfacial interactions or multiscale building blocks [23]. Recent investigations have demonstrated a great improvement in mechanical properties of GBNs via constructing different synergistic effects, as shown in Fig. 5. The mechanical properties of resultant GBNs, such as tensile strength, toughness, and Young's modulus, could be tuned through constructing a different combination of interfacial interactions or building blocks. The corresponding synergistic effects are discussed in detail in the following two sections.

### Synergistic effect from interfacial interactions

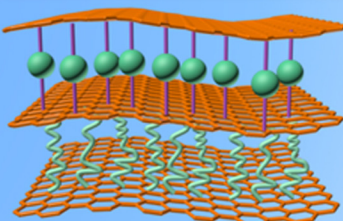
Based on the aforementioned interfacial interactions, there are six possible combination models: (i) hydrogen and ionic bonding; (ii) hydrogen bonding and  $\pi-\pi$  interaction; (iii) ionic bonding and  $\pi-\pi$  interaction; (iv) hydrogen and covalent bonding; (v) ionic and covalent bonding; and (vi)  $\pi-\pi$  interaction and covalent bonding. For example, Xu et al. [73] demonstrated the synergistic effect of hydrogen and ionic bonding in GBNs fiber via introducing the divalent ions of  $\text{Ca}^{2+}$ ,  $\text{Cu}^{2+}$  in the fabrication process. The tensile strength of resultant fiber GBNs reached up to 408.6 MPa, and 501.5 MPa for rGO-Cu<sup>2+</sup>, and rGO-Ca<sup>2+</sup>. Yan et al. [74] also demonstrated synergistic effect of hydrogen and ionic bonding by adding zirconium (Zr) into the layer-by-layer assembly of highly amorphous vinyl alcohol/reduced graphene oxide nanocomposites that resulted in a decrease of one order of magnitude of oxygen permeability. Zhang et al. [75] investigated the synergistic interfacial interactions of hydrogen bonding from hydroxypropyl cellulose and ionic bonding from copper ions in GBNs. Zhang et al. [76] demonstrated synergistic effect from hydrogen bonding and  $\pi-\pi$  interaction in GBNs. The poly(acrylic acid-co-(4-acrylamido-phenyl)boronic acid) (PAPB) was synthesized through grafting

## Synergistic effect from interfacial interactions

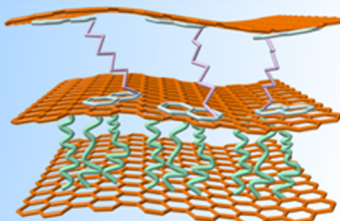
Hydrogen + covalent bonding



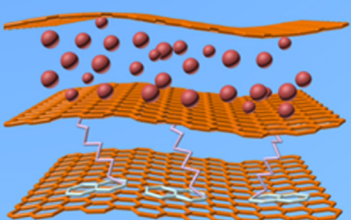
Ionic + covalent bonding



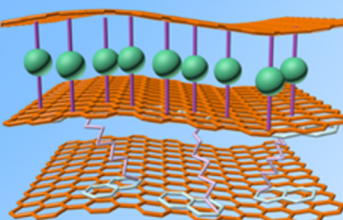
$\pi$ - $\pi$  interaction + covalent bonding



Hydrogen bonding +  $\pi$ - $\pi$  interaction

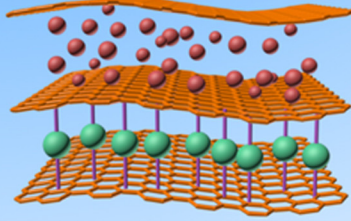


Ionic bonding +  $\pi$ - $\pi$  interaction



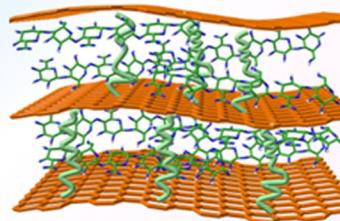
NFC

Hydrogen + ionic bonding

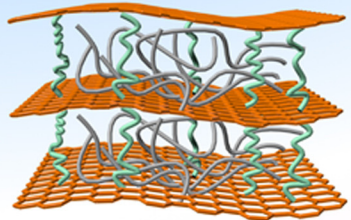


MoS<sub>2</sub>

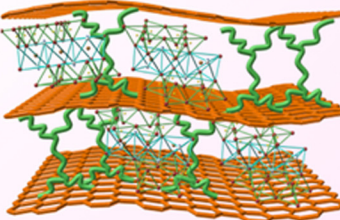
NFC + covalent bonding



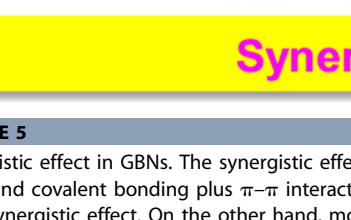
CNT + covalent bonding



WS<sub>2</sub> + covalent bonding



MMT + covalent bonding



## Synergistic effect from building blocks

FIGURE 5

Synergistic effect in GBNs. The synergistic effect from interfacial interactions is shown in cyan (upper left), including different combinations from hydrogen, ionic, and covalent bonding plus  $\pi$ - $\pi$  interactions. Integrated high strength and toughness GBNs have been demonstrated, revealing the amplification effect from synergistic effect. On the other hand, more complicated synergistic effects come from building blocks and interfacial interactions together, as shown in yellow (lower right), resulting in new functions besides enhancement of mechanical properties (e.g. high fatigue life and fire-retardant properties).

phenylboronic acid moieties into the side chains of poly(acrylic acid) (PAA), which formed the  $\pi-\pi$  interaction besides the hydrogen bonding between adjacent GO nanosheets. The resultant GBNs of rGO-PAPB show tensile strength of 382 MPa, and toughness of 7.5 MJ/m<sup>3</sup>, as well as electrical conductivity of 337 S/cm. Biomolecules, such as chitosan (CS) [77], and dopamine (DA) [72], are used to construct covalent bonding with adjacent GO nanosheets due to their many functional groups of hydroxyl and amine. Wan et al. [77] demonstrated the synergistic effect of hydrogen and covalent bonding in GBNs of CS-GO. The CS molecular chains can be placed on the surface of GO nanosheets via flow force, leading to exposure of buried reaction sites of amine. Then these active site groups react with carboxyl groups on the surface of GO nanosheets. When the optimized CS content is about 5.6 wt%, the synergistic effect from hydrogen and covalent bonding is achieved, resulting in a tensile strength of 526.7 MPa and toughness of 17.7 MJ/m<sup>3</sup>. Meanwhile, the electrical conductivity reaches 155.3 S/cm. Recently, Zhang et al. [15] also revealed the synergistic effect of ionic and covalent bonding in GBNs fiber. Ionic bonding is formed by Ca<sup>2+</sup>, and covalent bonding is constructed via a long chain linear molecule of PCDO. The synergistic effect is optimized through adjusting the ratio of

covalent bonding, resulting in a recorded tensile strength of 842.6 MPa, and high toughness of 15.8 MJ/m<sup>3</sup>. In addition, the electrical conductivity of this GBNs fiber reaches up to 292.4 S/cm. Recently, Gong et al. [78] also investigated the synergistic effect of ionic bonding with zinc and covalent bonding of PCDO molecule in GBNs.

### Synergistic effect from building blocks

Compared with interfacial interactions, the synergistic effect from building blocks in GBNs can be constructed with other nanomaterials, such as 1D nanofibers and 2D nanoplatelets. Furthermore, interfacial interactions can also be introduced with building blocks. For example, Xiong et al. [16] demonstrated a synergistic effect from 1D cellulose nanocrystals (CNCs) with GO nanosheets via a layer-by-layer (LBL) technique. The CNCs were modified with a cationic polyethyleneimine (PEI) to incorporate a positively charged surface to anionic GO nanosheets in LBL processing. Thus, ionic and hydrogen bonding were formed between GO nanosheets and a PEI modified CNCs network. These multiple synergistic effects resulted in a high tensile strength of 655 MPa and a record elastic modulus of 169 GPa, but low toughness.

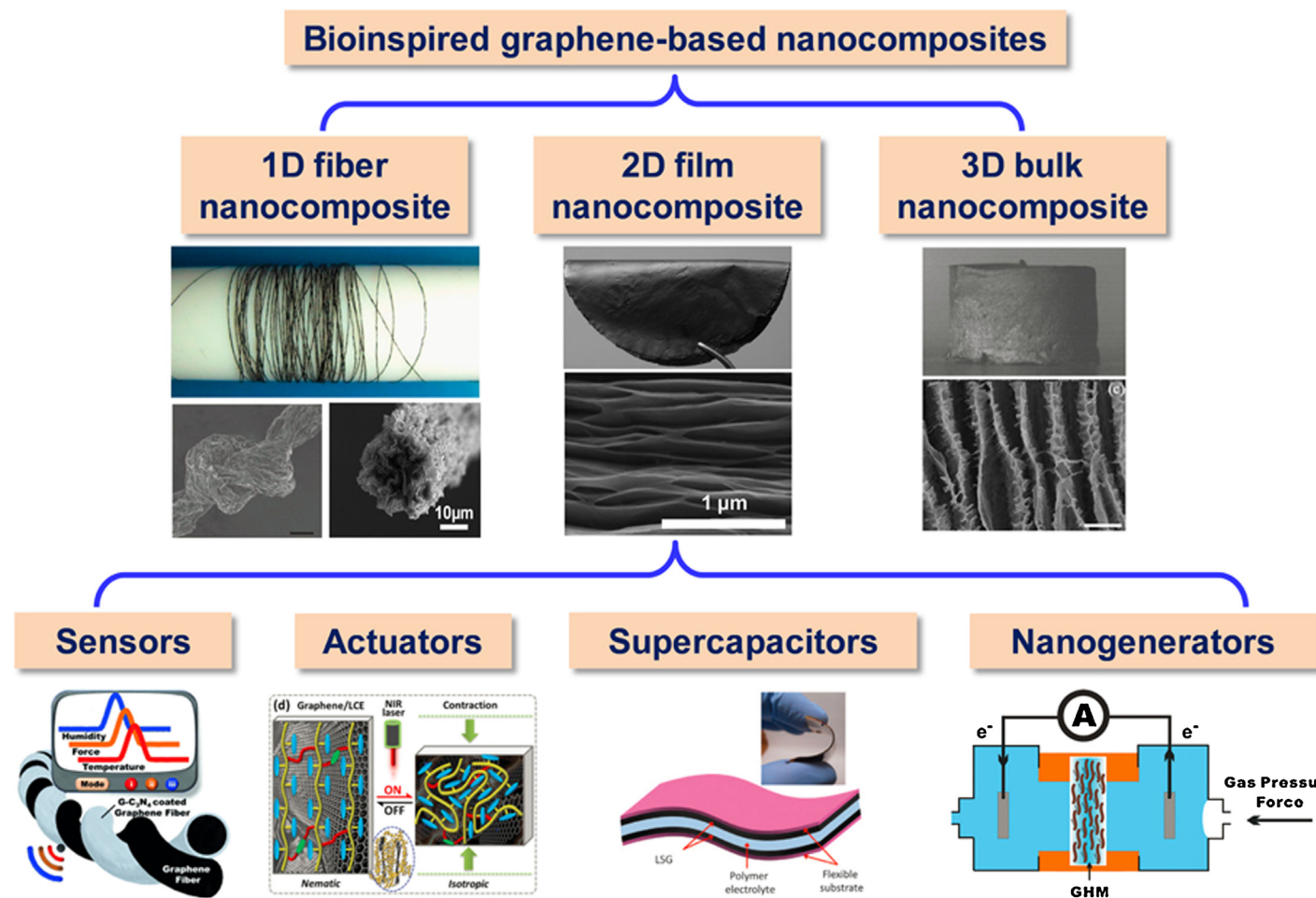


**FIGURE 6**

GBNs include three typical categories: 1D fiber, 2D film, and 3D bulk nanocomposites, which can be utilized in different applications, such as sensors (Reproduced from Ref. [81] with permission from Copyright © 2015 Wiley-VCH.), actuators (Reproduced from Ref. [82] with permission from Copyright © 2015 Wiley-VCH.), supercapacitors (Reproduced from Ref. [83] with permission from Copyright © 2012 The American Association for the Advancement of Science.), and nanogenerators (Reproduced from Ref. [84] with permission from Copyright © 2013 Wiley-VCH.).

Shin et al. [17] created high toughness of GBNs fiber via a synergistic effect from single-walled carbon nanotubes (SWNTs) and reduced graphene oxide flakes (RGOFs). Hydrogen bonding was formed between sodium dodecyl benzene sulfonate modified SWNTs and carboxyl groups on RGOFs. Meanwhile  $\pi-\pi$  interaction was also formed between oxygen-containing groups and aromatic regions with unoxidized benzene rings in RGOFs. These synergistic effects from SWNTs,  $\pi-\pi$  interaction, and hydrogen bonding together resulted in super high toughness of  $1380 \text{ MJ/m}^3$  for resultant SWNTs-RGOF-PVA nanocomposites. Recently, Gong et al. [79] realized the synergistic effect from 1D double-walled carbon nanotubes (DWNTs) and covalent bonding with GO nanosheets. The DWNTs content in resultant composites was optimized and covalent bonding of PCDO was simultaneously introduced. The bioinspired rGO-DWNTs-PCDO nanocomposites showed integrated mechanical properties, including high tensile strength, high toughness, and excellent fatigue life.

On the other hand, 2D nanoplatelets, such as montmorillonite (MMT), MoS<sub>2</sub>, and WS<sub>2</sub>, were also used to construct a synergistic effect with GO nanosheets. For example, the synergistic effect from lubrication of MoS<sub>2</sub> with GO nanosheets resulted in integrated ternary GBNs [33]. Besides the improvement in mechanical properties, the functions can be also achieved from a synergistic effect from building blocks, such as fire-retardant GBNs constructed through introducing MMT into GO-PVA nanocomposites [80].

## Applications

As already described, GBNs contain three kinds of typical assembly structure: (i) 1D fiber nanocomposites [5–8]; (ii) 2D film nanocomposites [2,9–12]; and (iii) 3D bulk nanocomposites [13,14]. GBNs with integrated mechanical and electrical properties have been demonstrated in many fields of flexible electronic devices (Fig. 6), such as sensors [81], actuators [82], supercapacitors [83], and nanogenerators [84]. For example, Zhao et al. [81] demonstrated multi-stimulus sensors based on graphene fiber nanocomposites, which were fabricated by twisting graphene fiber and graphitic carbon nitride coated graphene fiber (GF@GCN). The GF@GCN fiber nanocomposites were sensitive to slight temperature change, little force, and traces of moisture, as shown at lower left in Fig. 6. Yang et al. [82] showed a superior and tunable photomechanical actuator upon exposure to NIR irradiation, which was an assembled layered structure made of graphene and liquid crystal elastomer. Recently, high performance graphene nanocomposites-based supercapacitors were demonstrated [83,85]. The resultant supercapacitors maintain excellent electrochemical performance under high mechanical stress and high volumetric energy densities, and are promising candidates for flexible electronics devices. On the other hand, these GBNs can also be used as nanogenerators [84], as shown at lower right in Fig. 6. When electrolyte flow vertically through the graphene nanocomposites, the electrokinetic phenomenon happens, resulting in continuous and pulse-shaped ionic current signals.

## Conclusions and outlook

Natural materials, such as bamboo, bone, and nacre, provide a unique relationship between high mechanical performance and hierarchical micro/nanoscale architecture with abundant interfacial interactions. These inspirations have been demonstrated as a

'gold standard' for designing and fabricating artificial materials. Graphene and its derivatives show extraordinary physical properties, including mechanical and electrical properties, resulting in high performance GBNs [86], such as 1D fiber, 2D film, and 3D bulk nanocomposites.

By carefully controlling the precise hierarchical architecture and fine interfacial interactions, the physical performance of GBNs could be dramatically enhanced. In the near future, perhaps 5–10 years, the mechanical properties of GBNs will surpass those of carbon fiber reinforced composites, realizing practical applications in aerospace, aeronautics, submarine devices, car, and flexible electronic devices. For example, Xin et al. [21] adopted a strategy of using small-sized GO and large-sized GO to form an intercalated and compact fiber structure. After thermal annealing at  $2850^\circ\text{C}$ , the graphene fiber achieved thermal and electrical conductivities of  $1290 \text{ W/(m K)}$ , and  $2.21 \times 10^3 \text{ S/cm}$ , respectively, comparable to commercial carbon fiber. The tensile strength was as high as 1080 MPa. Recently, Xu et al. [87] presented a full scale synergistic defect engineering protocol to minimize possible defects and achieved graphene fibers with a stiffness of 282 GPa, tensile strength of 1.45 GPa, and electrical conductivity of  $0.8 \times 10^4 \text{ S/cm}$ , comparable to mechanical properties of carbon fiber and higher than the electrical conductivity of carbon fiber. GBNs are starting to make shifts from laboratory research to real-life applications, and novel integrated multifunctional properties are anticipated in the near future.

## Acknowledgements

This work was supported by the Excellent Young Scientist Foundation of NSFC (51522301), the National Natural Science Foundation of China (21273017 and 51103004), the Program for New Century Excellent Talents in University (NCET-12-0034), the Fok Ying-Tong Education Foundation (141045), the Open Project of Beijing National Laboratory for Molecular Sciences, the 111 Project (B14009), the Aeronautical Science Foundation of China (20145251035 and 2015ZF21009), the State Key Laboratory for Modification of Chemical Fibers and Polymer Materials, Donghua University (LK1508), the Key Research Program of the Chinese Academy of Sciences (KJZD-EW-M03), and the Fundamental Research Funds for the Central Universities (YWF-15-HHXY-001 and YWF-16-BJ-J-09).

## References

- [1] B. Su, et al. *J. Am. Chem. Soc.* 138 (2016) 1727.
- [2] Y. Zhang, et al. *Chem. Soc. Rev.* 45 (2016) 2378.
- [3] K. Hu, et al. *Prog. Polym. Sci.* 39 (2014) 1934.
- [4] U.G.K. Wegst, et al. *Nat. Mater.* 14 (2015) 23.
- [5] Z. Xu, et al. *Mater. Today* 18 (2015) 480.
- [6] Z. Xu, et al. *Acc. Chem. Res.* 47 (2014) 1267.
- [7] Z. Xu, et al. *Nat. Commun.* 2 (2011) 571.
- [8] F. Zhao, et al. *Mater. Today* 19 (2016) 146.
- [9] Y.L. Zhong, et al. *Mater. Today* 18 (2015) 73.
- [10] Q. Cheng, et al. *Angew. Chem. Int. Ed.* 52 (2013) 3750.
- [11] Q. Cheng, et al. *Acc. Chem. Res.* 47 (2014) 1256.
- [12] Q. Cheng, et al. *ACS Nano* 9 (2015) 2231.
- [13] P.C. Sherrell, et al. *Mater. Today* (2016), <http://dx.doi.org/10.1016/j.mattod.2015.12.004>.
- [14] L. Qiu, et al. *Nat. Commun.* 3 (2012) 1241.
- [15] Y. Zhang, et al. *Adv. Mater.* 28 (2016) 2834.
- [16] R. Xiong, et al. *Adv. Mater.* 28 (2015) 1501.
- [17] M.K. Shin, et al. *Nat. Commun.* 3 (2012) 650.

- [18] <http://www.carbonflyer.com/>.
- [19] X. Wang, et al. Environ. Eng. Sci. 8 (2015) 790.
- [20] Y. Yao, et al. ACS Nano 10 (2016) 5272.
- [21] G.Q. Xin, et al. Science 349 (2015) 1083.
- [22] M.A. Meyers, et al. Science 339 (2013) 773.
- [23] F. Barthelat, et al. Nat. Rev. Mater. 1 (2016) 16007.
- [24] H.D. Espinosa, et al. Prog. Mater. Sci. 54 (2009) 1059.
- [25] A. Jackson, et al. Proc. R. Soc. Lond. B: Biol. 234 (1988) 415.
- [26] J. Duan, et al. ACS Appl. Mater. Interfaces 8 (2016) 10545.
- [27] J. Wang, et al. ACS Nano 8 (2014) 2739.
- [28] X.Q. Li, et al. Adv. Mater. 24 (2012) 6277.
- [29] P. Podsiadlo, et al. Science 318 (2007) 80.
- [30] A.R. Studart, et al. Science 319 (2008) 1069.
- [31] H.-B. Yao, et al. Angew. Chem. Int. Ed. 49 (2010) 2140.
- [32] J.N. Coleman, et al. Science 331 (2011) 568.
- [33] S. Wan, et al. ACS Nano 9 (2015) 708.
- [34] Q. Cheng, et al. Adv. Mater. 24 (2012) 1838.
- [35] Y. Tian, et al. Nature 493 (2013) 385.
- [36] D.A. Dikin, et al. Nature 448 (2007) 457.
- [37] K.S. Novoselov, et al. Science 306 (2004) 666.
- [38] G.X. Li, et al. Chem. Commun. 46 (2010) 3256.
- [39] A. Brown, et al. Acta Cryst. 19 (1965) 684.
- [40] B. Ji, et al. J. Mech. Phys. Solids 52 (2004) 1963.
- [41] H. Sato, et al. J. Phys. Chem. B 105 (2001) 7990.
- [42] O.L. Manevitch, et al. J. Phys. Chem. B 108 (2004) 1428.
- [43] E. Munch, et al. Science 322 (2008) 1516.
- [44] I. Kaplan-Ashiri, et al. Proc. Natl. Acad. Sci. U.S.A. 103 (2006) 523.
- [45] S. Bertolazzi, et al. ACS Nano 5 (2011) 9703.
- [46] C.Y. Chan, et al. J. Cryst. Growth 247 (2003) 438.
- [47] C.-X. Wang, et al. Nanoscale 8 (2016) 901.
- [48] B. Peng, et al. Nat. Nanotechnol. 3 (2008) 626.
- [49] C. Lee, et al. Science 321 (2008) 385.
- [50] J.T. Paci, et al. J. Phys. Chem. C 111 (2007) 18099.
- [51] X. Wei, et al. Nat. Commun. 6 (2015) 8029.
- [52] J.W. Suk, et al. ACS Nano 4 (2010) 6557.
- [53] R.A. Soler-Crespo, et al. J. Phys. Chem. Lett. 7 (2016) 2702.
- [54] C. Cao, et al. Carbon 81 (2015) 497.
- [55] L. Liu, et al. Nanoscale 4 (2012) 5910.
- [56] S.W. Cranford, et al. Nanoscale 4 (2012) 7797.
- [57] S. Park, et al. Nat. Nanotechnol. 4 (2009) 217.
- [58] X.D. Wei, et al. ACS Nano 6 (2012) 2333.
- [59] H.D. Espinosa, et al. Nat. Commun. 2 (2011) 173.
- [60] F. Barthelat, et al. J. Mech. Phys. Solids 55 (2007) 306.
- [61] N.V. Medhekar, et al. ACS Nano 4 (2010) 2300.
- [62] K.W. Putz, et al. Adv. Funct. Mater. 20 (2010) 3322.
- [63] Y.-Q. Li, et al. Adv. Mater. 24 (2012) 3426.
- [64] O.C. Compton, et al. ACS Nano 6 (2012) 2008.
- [65] S. Park, et al. ACS Nano 2 (2008) 572.
- [66] Y. Xu, et al. J. Am. Chem. Soc. 130 (2008) 5856.
- [67] Y. Liu, et al. Nat. Commun. 5 (2014) 5461.
- [68] C.-C. Teng, et al. Carbon 49 (2011) 5107.
- [69] J. Zhang, et al. Composites Part A: Appl. Sci. Manuf. 71 (2015) 1.
- [70] Y. Gao, et al. ACS Nano 5 (2011) 2134.
- [71] Z. An, et al. Adv. Mater. 23 (2011) 3842.
- [72] W. Cui, et al. ACS Nano 8 (2014) 9511.
- [73] Z. Xu, et al. Adv. Mater. 25 (2013) 188.
- [74] N. Yan, et al. ACS Appl. Mater. Interfaces 7 (2015) 22678.
- [75] Q. Zhang, et al. Sci. China Technol. Sci. (2016) 1.
- [76] M. Zhang, et al. Adv. Mater. 26 (2014) 7588.
- [77] S. Wan, et al. ACS Nano 9 (2015) 9830.
- [78] S. Gong, et al. J. Mater. Chem. A (2016) 17073.
- [79] S. Gong, et al. ACS Nano 9 (2015) 11568.
- [80] P. Ming, et al. J. Mater. Chem. A 3 (2015) 21194.
- [81] F. Zhao, et al. Angew. Chem. Int. Ed. 54 (2015) 14951.
- [82] Y. Yang, et al. Adv. Mater. 27 (2015) 6376.
- [83] M.F. El-Kady, et al. Science 335 (2012) 1326.
- [84] W. Guo, et al. Adv. Mater. 25 (2013) 6064.
- [85] X.W. Yang, et al. Science 341 (2013) 534.
- [86] S. Wan, et al. Adv. Mater. (2016) 7862.
- [87] Z. Xu, et al. Adv. Mater. (2016) 6449.